https://doi.org/10.1016/j.nanoen.2015.12.001

Self-Powered Flat Panel Displays Enabled by Motion-Driven Alternating Current Electroluminescence

Huajing Fang[a], He Tian[b], Jing Li[a], Qiang Li[a], Jiyan Dai[c], Tian-Ling Ren[b], Guifang Dong[a], and Qingfeng Yan[a,*]

[a]*Department of Chemistry, Tsinghua University, Beijing100084, China*
[b]*Institute of Microelectronics, Tsinghua University, Beijing 100084, China*
[c]*Department of Applied Physics, The Hong Kong Polytechnic University, Hong Kong, China*
**Corresponding author. Qingfeng Yan (yanqf@mail.tsinghua.edu.cn)*

Abstract:
Self-powered systems have attracted significant attention in the past decades due to its independent and sustainable operations without other power source. In this work, a fully integrated self-powered flat panel display is proposed by coupling a ZnS powder based alternating current electroluminescence (ACEL) device and a built-in triboelectric nanogenerator (TENG). The built-in TENG was made of two different filtration membranes, avoiding conventional complicated nanostructure preparation process. This low-cost TENG can deliver a high output of V_{oc}=300V and I_{sc}=30μA, which is enough to directly turn on a light-emitting array. For the first time, a self-powered flexible ACEL device which might have great potential in intelligent electronic skin systems is demonstrated. The well matching between the electricity demand of ACEL and the output performance of TENG not only simplifies the supporting circuits but also saves the energy consumption on AC-DC transformation. These results indicate that the new motion-driven ACEL should have great potential towards the practical application of TENG in self-powered systems.

KEYWORDS: triboelectric nanogenerator; alternating current electroluminescence; finite element modeling; self-powered

Introduction

The massive development of electronic technology brings us a smart life. Self-powered system operating without bulky batteries and power cables is an emerging trend that may drive the world more intelligent and economy. In this regard, new approaches for green energy are urgently needed for independent, wireless and maintenance-free devices and systems [1-5]. Nanogenerators which can harvest mechanical energy from the environment as sustainable self-sufficient power source is a highly desired technology, as the mechanical energy is available almost everywhere around the clock [6-8]. Pioneered by Wang and co-workers in the last few years [9-12], nanogenerators based on different physical transduction mechanisms such as electromagnetic [13], electrostatic [14], piezoelectric [15] and triboelectric [16] have been developed. Since then, many different types of self-powered systems were demonstrated by using nanogenerators as the power source, including sensors [17-20], memories [21,22], electrochromic windows [23,24], cardiac pacemaker [25], UV sterilization [26], and other devices used in our daily life.

In a self-powered system, the generated electrical signal by nanogenerators can be converted to other signals (thermal, sound, light etc.), whereas electroluminescence (EL) is a nonthermal generation of light resulting from the application of an electric field. EL has been increasingly used as general illumination and displays, and there are two types of it. One is the familiar light-emitting diode (LED) device, which operates under relatively a low electric field and involves electron-hole recombination at the semiconductor p-n junctions. Powering commercial LEDs is a very common demonstrated application of nanogenerators in previous works [27-29]. Besides, Jeong and co-workers established a self-powered fully-flexible light emitting system composed of the AlGaInP vertically structured LEDs and a piezoelectric energy harvester [30]. Recently, we demonstrated a contact-electrification-gated LED by introducing triboelectric nanogenerator (TENG) into organic optoelectronics [31]. The other one is alternating current electroluminescence (ACEL), which was first discovered by Destrian et al. in ZnS compound [32]. Distinguished from the LEDs, ACEL device is usually called high-field EL, in which the light is generated by impact excitation of high energy electrons to luminescent center [33]. Due to their high resolution, uniform light emission, good contrast and brightness, ACEL devices have attracted great attentions in areas of liquid-crystal display backlighting and large-scale architectural and decorative lighting [34,35]. With the development of transparent electrodes, the ZnS powder-based ACEL has achieved great progress in recent years. Different transparent and conductive materials such as single-wall carbon nanotubes (SWCNT) [36], graphene [37], and Ag nanowires (NWs) [38] have been applied as substitutes of ITO to realize the flexible even stretchable ACEL devices. Among these transparent electrodes, Ag NWs stand out for their excellent optoelectronic performances along with the simple preparation process [39-42].

Although ACEL is the only mature technology for large-area flat or flexible light sources until now [43], their application in self-powered systems has rarely been reported yet. Very recently, Wei et al. [44] reported an isolated ACEL thin film on ITO glass which was connected to a TENG, forming a circuit without any electrical interface. The reduction of interface is particularly important not only to reduce the power consumption in circuit but also to shrink the size, weight and cost of the system. Based on this pioneer work, here we further demonstrate a fully integrated light-emitting array in which the ZnS powder based ACEL can be directly lighted on by finger taping a built-in TENG. Moreover, we also expand our self-powered display into flexible optoelectronic devices, which may have great potential in wearable electronics and electronic skin systems. The development of these applications is critical to the realization of artificial intelligent [45-47]. With the improved interaction between mechanical stimulus and luminescence, this work may open a window for developing self-powered displays and light sources.

Results and discussion

Figure 1 schematically illustrates the detailed structure of the self-powered flat panel display device. Printed circuit board (PCB) is chosen as the infrastructure because it is a mature industrial technology providing a cheap but reliable approach to orderly connect different electronic components [16]. To realize the contact and separation mode of TENG, at least one of the friction layers must be insulator. Here, polytetrafluoroethylene (PTFE) layer was attached on the lower PCB and served as one friction surface, taking advantage of its great

ability to gain electrons. Polyamide 6,6 (Nylon) layer was deposited as the opposite friction layer. On the top of this TENG, we prepared a 3×3 ZnS based ACEL arrays with cross-bar structure. Polydimethylsiloxane (PDMS) was used as polymer matrix for the light-emitting layer because of its low cost and simple preparation process. Transparent Ag NWs could be directly coated as front electrodes without concern of solvent compatibility problem which was hard to avoid in most organic EL devices [38]. At the same time, ACEL devices can work without strict requirements on the work functions matching between each layer of materials. It also provided a great advantage of easy fabrication compared to the LED. Finally, by connecting the ACEL arrays with the built-in TENG, the self-powered flat panel displays was established. The ACEL arrays could be driven by the electricity generated from the slight finger tapping on the TENG rather than other external energy sources.

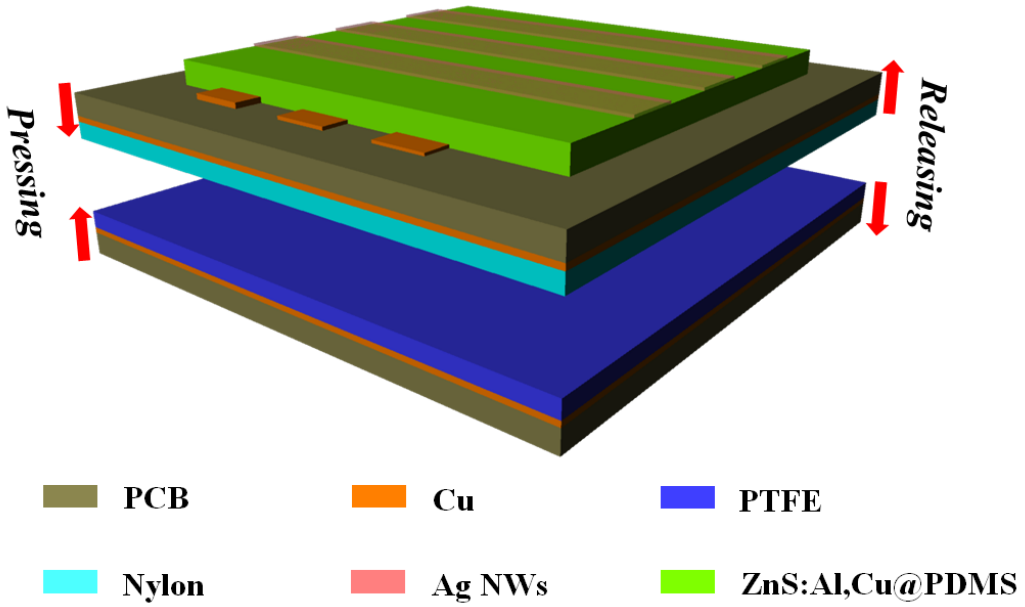

Figure 1 Schematic illustration of the self-powered flat panel displays, composed of a cross-bar structured ACEL array and a built-in TENG in vertical contact separation mode.

Ag NWs were used as the transparent front electrode in our ACEL device. Figure 2a presents the optical transmittance of the Ag NWs electrode. As shown, the average transmittance is nearly 85% in the visible range, comparable to the commercial ITO electrode. The inset image shows the photograph of the Ag NWs electrode coating on a glass coverslip, in which the text on the paper behind the coated glass is clearly visible. Figure 2b shows the SEM image of the uniform coating Ag NWs electrode. Meanwhile, the sheet resistance of this Ag NWs electrode can achieve ~30 Ω/□, which is comparable to the performance of ITO and meets the requirement for solar cell and other optoelectronic applications. To confirm the mixed state nature of the ZnS:Al,Cu powder and the PDMS polymer matrix, the cross-sectional SEM image of the light-emitting layer was acquired, as shown in Figure 2c. The ZnS:Al,Cu powders have been well dispersed in the PDMS matrix without any bubbles and voids. The complete coverage of PDMS over the phosphor particles can effectively avoid the catastrophic dielectric breakdown. Therefore, it is unnecessary to insert another dielectric layer between the rear electrode and the light-emitting layer as usual. X-ray powder

diffraction pattern is shown in Figure 2d. All the diffraction peaks can be assigned to a wurtzite structure (JCPDS no. 36-1450) of ZnS with good crystallinity.

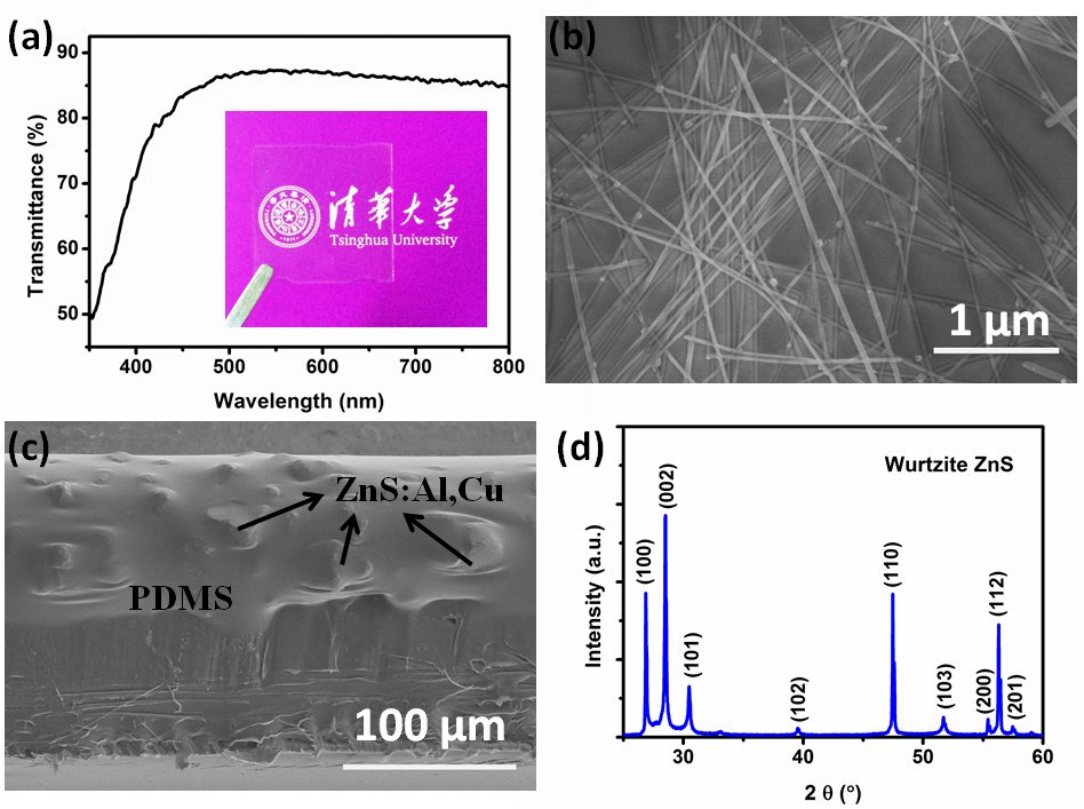

Figure 2 (a) Optical transmittance of the Ag NWs electrode. Image in the inset is a photograph of the Ag NWs electrode coating on a glass coverslip (24 ×24 mm). (b) SEM image of the Ag NWs coating on a glass coverslip. (c) Cross-sectional SEM image of the light-emitting layer. (d) X-ray diffraction pattern of the ZnS:Al,Cu powder.

To assess the performance of the fabricated powder based ACEL arrays, a single element was driven by a sinusoidal power as shown in Figure 3a. Electroluminescence spectra at varied applied voltages varying from 100 to 300 V at a fixed frequency of 70 Hz are shown in Figure 3b. The dominant peak of luminescence spectrum is seen at 508 nm, and a minor shoulder band can also be found at 460 nm. These spectra features can be understood by the donor-acceptor (D-A) type emission process as schematically shown in Figure 3c. The sulphur vacancies (Vs) caused by the lattice dislocation and the Al^{3+} substitution to Zn^{2+} site (Al_{Zn}) can separately generate two different donor levels below the conduction band (CB). The acceptor level above the valance band (VB) was generated by the Cu^{+} substitution to Zn^{2+} site (Cu_{Zn}). Thus, the dominant peak at 508 nm (2.42 eV) can be assigned to the D-A recombination of Al_{Zn}-Cu_{Zn} in the energy level diagram, and the shoulder band at 460 nm (2.70 eV) originates from the D-A recombination of V_S-Cu_{Zn} [48]. The emission intensity against the applied voltage is plotted in the inset of Figure 3b. The ACEL element initiates light emission at 100 V and the emission intensity increases rapidly with the increasing applied voltage. As known, the relation between the EL intensity and the applied voltage can be evaluated by the following equation [38]:

$$L = L_0 \exp(-\beta/V^{1/2})$$

Where L is the luminance, V is the applied voltage, while L_0 and β are the constants determined by the phosphor material and device structure [49]. The CIE coordinate of the device obtained simultaneously with the EL spectrum is (0.1882, 0.3742). It corresponds to a typical green emission, as shown in Figure 3d.

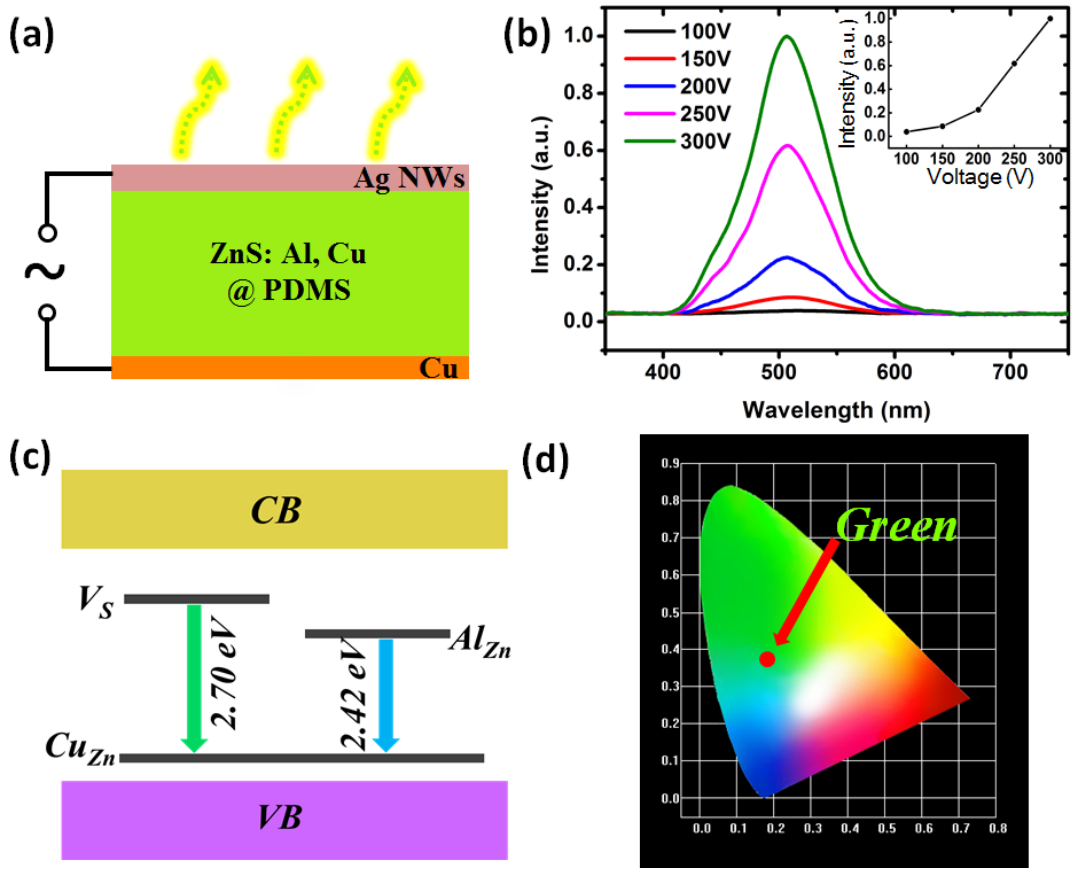

Figure 3 (a) Device structure of a single ACEL element. (b) Electroluminescence spectrum of a single ACEL element operating at 70 Hz with different voltages. The emission intensity at 508 nm as a function of applied voltage is shown in the inset. (c) Energy level diagram of ZnS:Al,Cu phosphor. (d) The CIE diagram showing the green light emitting from the ACEL element.

On the other hand, Nylon and PTFE were purposely chosen as the friction layers to fabricate the built-in TENG, because these two polymers were at the opposite ends of the triboelectric series [50]. It has been demonstrated that micro/nanostructures existing on the surface of friction layers can contribute to higher performance of a TENG. Hence, different preparation methods including photolithography, dry-etching, and block copolymer self-assembly have been used to increase the surface roughness on the contact surface of TENG in previous works [5,50,51]. While in this work, the fabrication of TENG does not rely on any expensive equipment or complex procedures mentioned before. Because both PTFE and Nylon happen to be the common materials of filtration membranes which have ready-made nanostructures as shown in Figure 4. The dense nanostructures can not only enlarge the surface area, but also enhance the rubbing between each other. By a clever use of these two different filtration membranes, we designed a low-cost TENG below the ACEL device as shown in Figure 1.

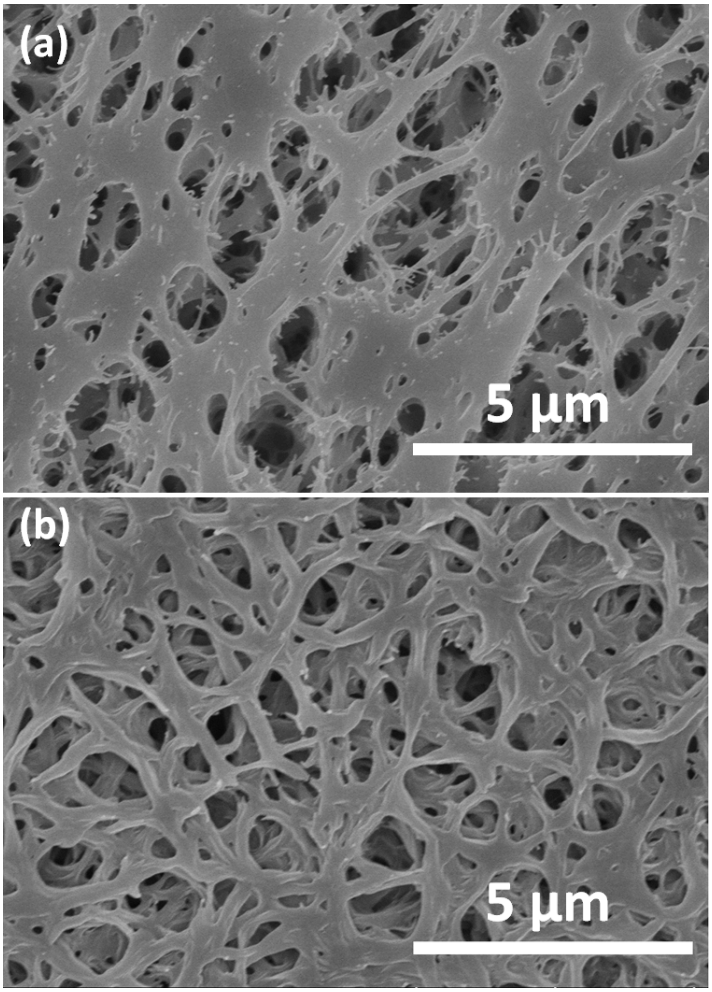

Figure 4 Top view SEM images of (a) the PTFE surface and (b) the Nylon surface with nanostructures.

Next, the electric output performance of the built-in TENG under a periodical finger tapping was tested. The measured open-circuit voltage (V_{oc}) in the forward connection shows a peak value of about 300 V, as seen in Figure 5a. As shown in Figure 5b, switching polarity test under a reverse connection mode gives almost the same amplitude but reversed polarity. This phenomenon confirms the validity of the output signals. Figure 5c shows that the short-circuit current (I_{sc}) with a resistance of 2 MΩ can reach 30 µA. The enlarged view of the output current over a single cycle is shown in Figure 5d, where one can see that the positive signal has a much larger peak value (30 µA) but a shorter pulse compared to a much smaller peak value (10 µA) but a longer pulse in the negative signal. This feature is caused by the different straining rates during the pressing and releasing stages. As we know, the amount of transferred charge (Q) is the time integral of current ($Q = \int I\, dt$). Actually, it can be observed from the purple line in Figure 5d that Q remains the same (90 nC) in both pressing and releasing stages. Taking the contacting area of 19.26 cm^2 into account, the output charge density reaches ~ 46µC/m^2. Hence, the nature of the electricity generated in the TENG is the alternating flow of these induced charges.

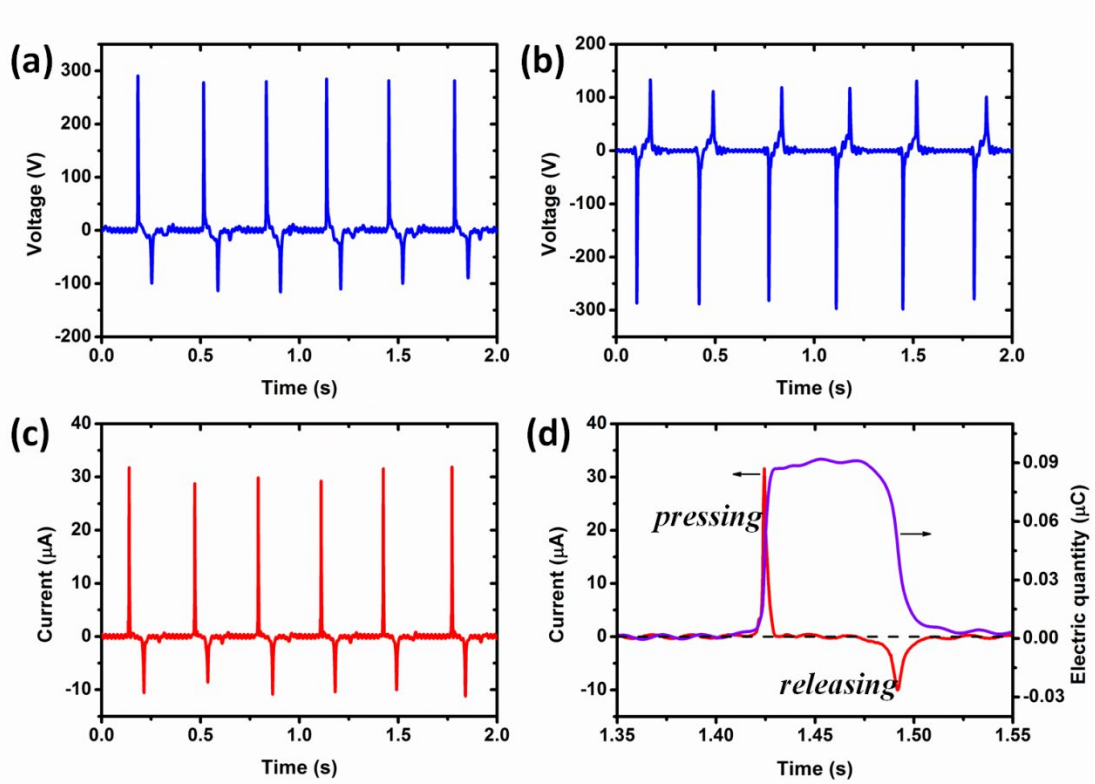

Figure 5 Performance of the built-in TENG during the periodical finger tapping motions. (a) The open-circuit voltage V_{oc} in the forward connection and (b) The open-circuit voltage in reversed connection. (c) The short-circuit current I_{sc} signals in the forward connection. (d) The enlarged view of the short-circuit current and transferred charge over a single tapping cycle.

After the individual characterization of the ACEL and TENG, a concurrent operation of the two parts was performed to demonstrate the working principle of a self-powered flat panel display. As expected, when two electrodes of the built-in TENG were connected to the ACEL device, the alternating flow of induced charges can generate an AC electric field across the light-emitting layer. In order to further understand this, we calculated the distribution of the instantaneous electric field inside the light-emitting layer by a finite element modeling (FEM, via Comsol Multiphysics). Figure 6 represents a simulated model whose geometry parameters are from real device. The thickness of this light-emitting layer is ~ 80 μm, see Figure 2c. And ZnS:Al,Cu phosphor powders are equivalent to microspheres with an average diameter of 35 μm for simplifying the model. The simulated potential and electric field distribution in the light-emitting layer are shown in Figure 6a and b respectively. Due to the difference of relative permittivity between the ZnS based phosphor and the PDMS polymer matrix, the electric field distribution in the light-emitting layer is not uniform. The calculated results demonstrate that the local electric field in phosphors is up to the order of 10^6 V/m, which is enough to accelerate electrons in ZnS:Al,Cu powder and excite luminescence. These results support the feasibility of the designed self-powered microelectromechanical systems (MEMS).

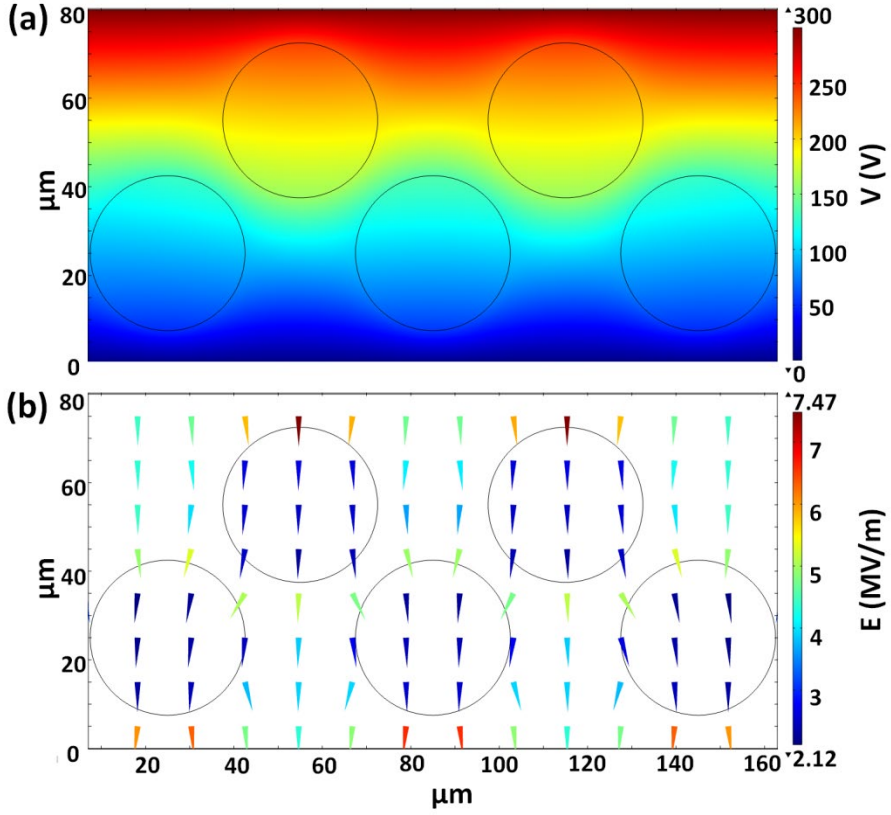

Figure 6 Numerically calculated (a) potential and (b) electric field distribution in the light emitting layer driven by the built-in TENG.

Figure 7a shows the measured luminescence spectra of the ACEL arrays under finger tapping the TENG without any external power supply. The main peak locates at 514 nm and the shoulder band almost disappears. The slight changes in peak position compared to the EL spectra shown in Figure 3b is attributed to the difference of applied frequency, as there is a strong dependence of emission intensity and color on the applied frequency [36]. In Figure 7b, a 3 ×3 ACEL array being simultaneously turned on by finger tapping a built-in TENG is shown (also see Video 1 in the Supporting Information). As we can see, the integrated device can effectively convert the input mechanical energy to light energy by the coupling effects between triboelectric and ACEL. This strategy is fundamentally different from the mechanoluminescence (ML) in the same ZnS material system reported previously [52-55]. As in those works, piezoelectric potential caused by the external strain is capable of triggering the luminescent center of metal-ion dopants, leading to light emissions. Compared to the ML which always requires large strain and difficult to achieve large-area light emitting, our devices can suit more accessible mechanical stimulus and have a larger emitting face (2.25 cm^2). We further expanded our self-powered display into flexible optoelectronic devices, which may have great potential in intelligent electronic skin systems. Figure 7c shows a bending ACEL device attached on top of a finger. As seen in Figure 7c, it can also be turned on by the TENG successfully. Compared to the LEDs, the ACEL device does not need the AC-DC converter, because its luminescence can be excited by the high electric field regardless of polarity. Hence, as shown in Figure 7d, the ACEL device can be turned on twice

in every pressing - releasing cycle, more details can be found in Video 1 in the Supporting Information. While the commercial LEDs can only be turned on once, similar results can be found in AlGaInP vertically structured LEDs reported by Jeong et al. [30]. The well matching between the electricity demand of ACEL and the output characteristics of TENG (AC high voltage) can not only simplify the supporting circuits but also save the energy consumed on AC-DC transformation. These results fully demonstrate that the high-performance TENG can serve as a reliable energy supplier for self-powered flat panel display.

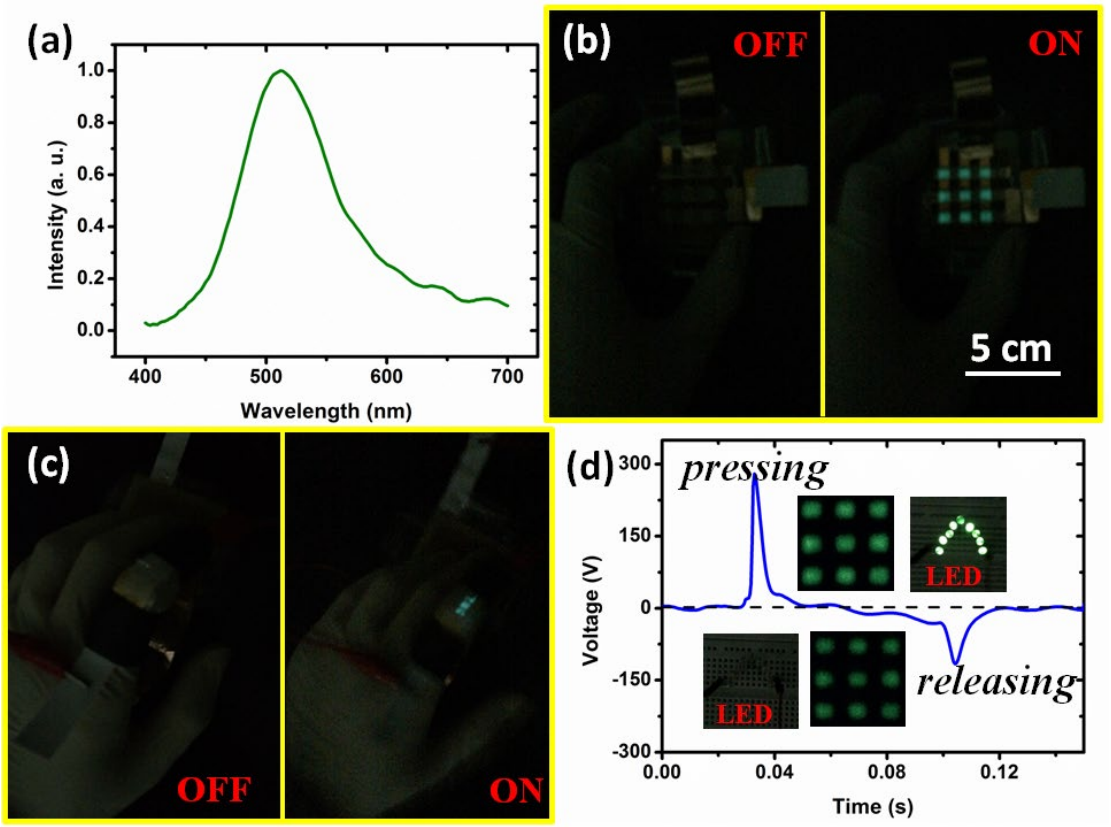

Figure 7 (a) Luminescence spectra of the motion-driven ACEL arrays under finger tapping of a built-in TENG. (b) Photographic image of the self-powered flat panel displays. (c) Photographic image of the self-powered flexible ACEL device. (d) The luminescence of the device during pressing-releasing cycles, compared to the commercial green LEDs.

Conclusions

To conclude, the concept of a motion-driven self-powered flat panel display has been realized by the full integration of an ACEL array and a built-in triboelectric nanogenerator. The green light-emitting ZnS powder based ACEL devices have been successfully fabricated on both rigid and flexible substrates. By a clever use of two different organic filtration membranes, a high-performance TENG has been produced without any expensive equipment or complex procedure. During repeated finger tapping motions, the output voltage of TENG (as high as 300 V) can generate an instantaneous electric field which is enough to excite luminescence of ZnS:Al,Cu powder. This work demonstrates the feasibility of self-powered flat panel display and shows great potential towards the practical application of TENG in self-powered MEMS.

Experimental section

Fabrication of the self-powered flat panel displays

Two pieces of PCB were designed and prepared with the copper pattern grating embedded into the stiff glass epoxy base materials. This industrial technology paves the way for large-scale production and the following integration of two functional devices. The ACEL array was prepared as follows: ZnS:Al,Cu powder (GGS42, Global Tungsten & Powders Co.) were first uniformly mixed in PDMS (Sylgard184, Dow Corning) pre-polymer with a weight ratio of 7:3. After degassing for 30 min, the mixture was deposited on the Cu pattern by screen-printing. Subsequent curing was done at 100 ^{o}C for 2h. Finally, Ag NWs electrodes were coated on the cured emitting layer with designed patterns. To build up the self-powered flat panel displays shown in Figure1, Nylon layer was deposited on the bottom of the prepared ACEL array as one friction layer. PTFE layer was attached on another PCB as the opposite friction layer. The built-in contact-separation mode TENG was achieved by packing these two friction layer face to face.

Characterization

The optical transmission of Ag NWs transparent electrode was measured using a UV-visible spectrophotometer (HITACHI, U-3010), whereas the sheet resistance (Rs) was measured by the four point probe sheet resistance meter (Dimensions, 280SJ). All the SEM images were taken on the field-emission scanning electron microscopy (FESEM, JEOL JSM-6335F). The crystal structures of the metal ion doped ZnS powder were characterized through X-ray diffraction (XRD, Bruker D8-Advance) using Cu Kα radiation. The EL spectra were carried out by a spectrophotometer (Edinburgh, FLSP920) with different AC voltage at the frequency of 70 Hz. The output signal of the built-in TENG was recorded by the digital multimeter (RIGOL DM3068) under mechanical tapping. The self-powered flat panel displays were characterized by recording the luminescence spectra using an Ocean Optics USB4000 CCD spectrometer with the continuous finger tapping on the built-in TENG.

Acknowledgments

The authors thank Prof. Zhiguo Xia for his fruitful discussion. This research was supported by the National key Basic Research Program of China (973 Program) under Grant No. 2013CB632900, and the National Science Foundation of China (No. 51173097, 91333109, 61574083 and 61434001). The Tsinghua University Initiative Scientific Research Program (No. 20131089202), the Open Research Fund Program of the State Key Laboratory of Low-Dimensional Quantum Physics (No. KF201516) and the Hong Kong Polytechnic University strategic plan (No: 1-ZVAW and 1-ZVCG) are also acknowledged for partial financial support.

Appendix A. Supporting information

Supplementary data associated with this article can be found in the online version at...

References

[1] Y.F. Hu, Z.L. Wang, Nano Energy 14 (2015) 3-14.

[2] Z.L. Wang, J. Chen, L. Lin, Energy Environ. Sci. 8 (2015) 2250-2282.

[3] C.R. Bowen, H.A. Kim, P.M. Weaver, S. Dunn, Energy Environ. Sci. 7 (2014) 25-44.
[4] Z.L. Wang, ACS Nano 7 (2013) 9533-9557.
[5] B Meng, W. Tang, Z. Too, X.S. Zhang, M.D. Han, W. Liu, H.X. Zhang, Energy Environ. Sci. 6 (2013) 3235-3240.
[6] K. Park, C.K. Jeong, J. Ryu, G.T. Hwang, K.J. Lee, Adv. Energy Mater. 3 (2013) 1539-1544.
[7] C. Chang, V.H. Tran, J. Wang, Y.K. Fuh, L. Lin, Nano Lett. 10 (2010) 726-731.
[8] B. Kumar, S.W. Kim, J. Mater. Chem. 21 (2011) 18946-18958.
[9] X.D. Wang, J.H. Song, J. Lin, Z.L. Wang, Science, 6 (2007) 102-105.
[10] S. Xu, Y. Qin, C. Xu, Y.G. Wei, R.S. Yang, Z.L. Wang, Nat. Nanotech. 5 (2010) 366-373.
[11] S. Xu, B.J. Hansen, Z.L. Wang, Nat. Common. 1 (2010) 93.
[12] Z.L. Wang, Adv. Funct. Mater. 18 (2008) 3553-3567.
[13] Y. Wu, X. Wang, Y. Yang, Z.L. Wang, Nano Energy 11 (2015) 162-170.
[14] H. Tian, S. Ma, H.M. Zhao, C. Wu, J. Ge, D. Xie, Y. Yang, T.L. Ren, Nanoscale 5 (2013) 8951-8957.
[15] A. Koka, Z. Zhou, H.A. Sodano, Energy Environ. Sci. 7 (2014) 288-296.
[16] X.S. Zhang, M.D. Han, B. Meng, H.X. Zhang, Nano Energy 11 (2015) 304-322.
[17] H.J. Fang, Q. Li, J. Ding, N. Li, H. Tian, L.J. Zhang, T.L. Ren, J.Y. Dai, L.D. Wang, Q.F. Yan, (2016) DOI: 10.1039/C5TC03342J.
[18] Y.B. Zheng, L. Cheng, M. Yuan, Z. Wang, L. Zhang, Y. Qin, T. Jing, Nanoscale 6 (2014) 7842-7846.
[19] H. Guo, J. Chen, L. Tian, Q. Leng, Y. Xi, C.G. Hu, ACS Appl. Mater. Interfaces 6 (2014) 17184-17189.
[20] B. Saravanakumar, S. Soyoon, S.J. Kim, ACS Appl. Mater. Interfaces 6 (2014) 13716-13723.
[21] H.J. Fang, Q. Li, W.H. He, J. Li, Q.T. Xue, C. Xu, L.J. Zhang, T.L. Ren, G.F. Dong, H. L. W. Chan, J.Y. Dai, Q.F. Yan, Nanoscale, 7 (2015) 17306-17311.
[22] X.Y. Chen, M. Iwamoto, Z.M. Shi, L.M. Zhang, Z.L. Wang, Adv. Funct. Mater. 25 (2015) 739-747.
[23] M.H. Yeh, L. Lin, P.K. Yang, Z.L. Wang, ACS Nano 9 (2015) 4757-4765.
[24] X.H. Yang, G. Zhu, S.H. Wang, R. Zhang, L. Lin, W.Z. Wu, Z.L. Wang, Energy Environ. Sci. 5 (2012) 9462-9466.
[25] G.T. Hwang, H. Park, J.H. Lee, S. Oh, K. Park, M. Byun, H. Park, G. Ahn, C.K. Jeong, K. No, H. Kwon, S.G. Lee, B. Joung, K.J. Lee, Adv. Mater. 26 (2014) 4880-4887.
[26] C.B. Han, C. Zhang, J. Tian, X. Li, L. Zhang, Z. Li, Z.L. Wang, Nano Res. 8 (2015) 219-226.
[27] M.D. Han, X.S. Zhang, B. Meng, W. Liu, W. Tang, X.M. Sun, W. Wang, H.X. Zhang, ACS Nano 7 (2013) 8554-8560.
[28] J.W. Zhong, Q. Zhong, F.R. Fan, Y. Zhang, S.H. Wang, B. Hu, Z.L. Wang, J. Zhou, Nano Energy 2 (2013) 491-497.
[29] Q. Leng, H.Y. Guo, X.M. He, G.L. Liu, Y. Kang, C.G. Hu, Y. Xi, J. Mater. Chem. A 2 (2014) 19427-19434.
[30] C.K. Jeong, K. Park, J.H. Son, G.T. Hwang, S.H. Lee, D.Y. Park, H.E. Lee, H.K. Lee, M. Byun, K.J. Lee, Energy Environ. Sci. 7 (2014) 4035-4043.

[31] C. Zhang, J. Li, C.B. Han, L.M. Zhang, X.Y. Chen, L.D. Wang, G.F. Dong, Z.L. Wang, Adv. Funct. Mater. 25 (2015) 5625-5632.
[32] G. Destriau, J. Chemie Physique 33 (1936) 587-625.
[33] R. Withnall, J. Silver, P.G. Harris, T.G. Ireland, P.J. Marsh, J. SID 19 (2011) 798-810.
[34] J.H. Park, S.H. Lee, J.S. Kim, A.K. Kwon, H.L. Park, S.D. Han, J. Lumin. 126 (2007) 566-570.
[35] V.I. Vlaskin, S.I. Vlaskina, O.Y. Koval, V.E. Rodionov, G.S. Svechnikov, Semicond. Phys., Quantum Electron. Optoelectron. 10 (2007) 16-20.
[36] C. Schrage, S. Kaskel, ACS Appl. Mater. Interfaces 1 (2009) 1640-1644.
[37] Z. Wang, Y. Chen, P. Li, X. Hao, J. Liu, R. Huang, Y. Li, ACS Nano 5 (2011) 7149-7154.
[38] J. Wang, C. Yan, K.J. Chee, P.S. Lee, Adv. Mater. 27 (2015) 2876-2882.
[39] F. Xu, Y. Zhu, Adv. Mater. 24 (2012) 5117-5122.
[40] X.Y. Zeng, Q.K. Zhang, R.M. Yu, C.Z. Lu, Adv. Mater. 22 (2010) 4484-4488.
[41] S. De, T.M. Higgins, P.E. Lyons, E.M. Doherty, P.N. Nirmalraj, W.J. Blau, J.J. Boland, J.N. Coleman, ACS Nano 3 (2009) 1767-1774.
[42] L. Hu, H.S. Kim, J.Y. Lee, P. Peumans, Y. Cui, ACS Nano 4 (2010) 2955-2963.
[43] M. Bredol, H. S. Dieckhoff, Materials 3 (2010) 1353-1374.
[44] X.Y. Wei, S.Y. Kuang, H.Y. Li, C. Pan, G. Zhu, Z.L. Wang, Sci. Rep. 5 (2015) 13658.
[45] Z. Chen, J.W.F. To, C. Wang, Z. Lu, N. Liu, A. Chortos, L. Pan, F. Wei, Y. Cui, Z.N. Bao, Adv. Energy Mater. 4 (2014) 1400207.
[46] S.C.B. Mannsfeld, B.C.K. Tee, R.M. Stoltenberg, C.V.H.H. Chen, S. Barman, B.V.O. Muir, A.N. Sokolov, C. Reese, Z.N. Bao, Nat. Mater. 9 (2010) 859-864.
[47] G. Schwartz, B.C.K. Tee, J. Mei, A.L. Appleton, D.H. Kim, H. Wang, Z.N. Bao, Nat. Common. 4 (2013) 1859.
[48] L. Chen, M.C. Wong, G. Bai, W. Jie, J.H. Hao, Nano Energy 14 (2015) 372-381.
[49] B. Qiao, Z.L. Tang, Z.T. Zhang, L. Chen, Mater. Lett. 61 (2007) 401-404.
[50] S. Wang, L. Lin, Y. Xie, Q. Jing, S. Niu, Z.L. Wang, Nano Lett. 13 (2013) 2226-2233.
[51] C.K. Jeong, K.M. Baek, S. Niu, T.W. Nam, Y.H. Hur, D.Y. Park, G.T. Hwang, M. Byun, Z.L. Wang, Y.S. Jung, K.J. Lee, Nano Lett. 14 (2014) 7031-7038.
[52] S.M. Jeong, S. Song, S.K. Lee, B. Choi, Appl. Phys. Lett. 102 (2013) 051110.
[53] S.M. Jeong, S. Song, S.K. Lee, N.Y. Ha, Adv. Mater. 25 (2013) 6194-6200.
[54] X. Wang, H. Zhang, R. Yu, L. Dong, D. Peng, A. Zhang, Y. Zhang, H. Liu, C Pan, Z.L. Wang, Adv. Mater. 27 (2015) 2324-2331.
[55] M.C. Wong, L. Chen, M.K. Tsang, Y. Zhang, J.H. Hao, Adv. Mater. 27 (2015) 4488-4495.

Huajing Fang is currently a Ph.D. candidate under the supervision of Prof. Qingfeng Yan in Department of Chemistry, Tsinghua University. He was also a research assistant in Department of Applied Physics, Hong Kong Polytechnic University in 2013-2014. His research interests focus on the application of piezoelectric materials and self-powered systems.

He Tian received his Ph.D. degree in the Institute of Microelectronics from Tsinghua University. He was also a visiting researcher at Lawrence Berkeley National Laboratory in 2012. Now he is a Postdoctoral Scholar of University of Southern California and Postdoctoral Fellow of Yale University. His research interest is novel devices based on 2D materials.

Jing Li is currently a master degree candidate in the Department of Chemistry, Tsinghua University, under the supervision of Prof. Gui-Fang Dong. Her research focuses on the organic thin-film transistors.

Prof. Qiang Li received his Ph.D. degree on materials science from Wuhan University of Technology in 1993 and was promoted to professor in 1995. He moved to the Department of Chemistry at Tsinghua University as a professor in 2000. His research interests mainly focus on crystal materials & crystal growth, crystallology, ferroelectric (anti-ferroelectric) materials and related functional materials synthesis etc.

Prof. Ji-yan Dai received his Ph.D. degree in Materials Physics from the Chinese Academy of Sciences in 1994. Since 1995, he has done postdoctoral research work at Northwestern University (USA) and the Institute of Materials Research and Engineering (Singapore), and then worked in Chartered Semiconductor Manufacturing Ltd. of Singapore as a principle engineer. Prof. Dai joined Department of Applied Physics, The Hong Kong Polytechnic University, in 2001. His main research area is the study of structure and device applications of functional oxide thin films and medical ultrasound transducers with new materials.

Tian-Ling Ren is full professor of Institute of Microelectronics, Tsinghua University since 2003. He received his Ph.D. degree in solid-state physics from Department of Modern Applied Physics, Tsinghua University, China in 1997. His main research interests include new material based micro/nano devices and systems, flexible electronics, non-volatile memory, etc. He has published 300 journal and conference papers for these years.

Dr. Gui-Fang Dong received her Ph.D. degree from the Department of Electronic Engineering, Tsinghua University in 2000. Then she joined Department of Chemistry, Tsinghua University as an interdisciplinary researcher. Currently, she is an associate professor. Her research focuses on organic transistors, organic photodiodes and organic optocouplers.

Dr. Qingfeng Yan received his Ph.D. degree from the Institute of Semiconductors, Chinese Academy of Sciences in 2003. He joined the Department of Chemical & Biomolecular Engineering, National University of Singapore as a research fellow in 2003. From 2006, he worked with the School of Materials Science and Engineering, Nanyang Technological University and the Department of Materials Science and Engineering, Massachusetts Institute of Technology as a joint postdoctoral fellow. He joined the Department of Chemistry, Tsinghua University as an associate professor in 2008. His current research interest focuses on synthetic single crystals and chemical self-assembly approach to functional thin films.